3) Henry, E. J. and E. M. Rosen: "Material and Energy Balance Computations," p. 202, Wiley, New York (1969).
4) Hirai, H., M. Komiyama and S. Hara: *Makromol. Chem. Rapid Commun.*, **2**, 495 (1981).
5) Kitagawa, H. and A. Inoue: *Nenryou Kyoukaishi*, **45**, 110 (1966).
6) Larson, A. T. and C. S. Teithworth: *J. Am. Chem. Soc.*, **44**, 2878 (1922).
7) Loprest, F. J.: *J. Phys. Chem.*, **61**, 1128 (1957).
8) Stephen, H. and T. Stephen: "Solubilities of Inorganic and Organic Compounds," Vol. 1, Part 2, p. 1053, Pergamon Press (1963).
9) Turner, R. W. and E. L. Amma: *J. Am. Chem. Soc.*, **88**, 187 (1966).
10) Westerterp, K. R., W. P. M. van Swaaij and A. A. C. M Beenackers: "Chemical Reactor Design and Operation", 2nd ed., p. 377, Wiley, New York (1984).

(Presented at Hokkaido Meeting of The Society of Chemical Engineers, Japan at Sapporo, July, 1987.)

EFFECT OF ANODIC AND CATHODIC REACTIONS ON OXIDATIVE DEGRADATION OF PHENOL IN AN UNDIVIDED BIPOLAR ELECTROLYZER

MASAO SUDOH, TAKAMASA KODERA, HARUYOSHI HINO AND HIROSHI SHIMAMURA

Department of Chemical Engineering, Shizuoka University, Hamamatsu 432

Key Words: Electrolysis, Bipolar Electrode, Oxidative Degradation, Phenol, Current Efficiency

Both anodic oxidation and generation of hydrogen peroxide through electroreduction of oxygen may be useful for oxidative degradation of organic compounds. To clarify the effect of electrode reactions of both sides of a bipolar plate on the current efficiency for oxidative degradation of phenol, experiments were conducted by using an undivided bipolar electrolyzer having a vertical stack of perforated graphite electrodes. The Faradaic current I_f was arranged as a function of the electrode potential difference E_B between opposite sides of a bipolar plate. By analyzing the $I_f - E_B$ curves for the electrolyses in solutions containing different reactants, separate currents corresponding to anodic and cathodic reactions were determined. The effect of E_B on the COD current efficiency *Ce*(COD) for the oxidative degradation of phenol could be well explained by the contribution of the currents of phenol oxidation and oxygen reduction to the total current. The value of *Ce*(COD) in case of sparging oxygen showed a bimodal curve having the maximum values with respect to E_B.

Introduction

Electrochemical treatments of waste water containing organic compounds are classified into two groups: direct oxidation on the anode and indirect oxidation using an oxidizing agent, hypochlorite[2] or hydrogen peroxide, which is produced by electrolysis.[5] Hydrogen peroxide is produced through electroreduction of oxygen on the cathode.[7,8] In our previous paper,[9] the oxidative degradation of aqueous phenol effluent with electrogenerated Fenton's reagent in a catholyte compartment separated by a membrane in an H-type cell was reported. In the ideal case, both anodic oxidation and cathodic reduction in an undivided cell may be useful for oxidative degradation.

Received July 30, 1987. Correspondence concerning this article should be addressed to M. Sudoh. T. Kodera is now at Nippon Steel Corp. Ltd., Tokai 476.

In the present work, a divided bipolar electrolyzer having a vertical stack of perforated graphite electrodes is used experimentally to clarify the effect of both electrode reactions on total current efficiency for the oxidative degradation of phenol. The current-voltage curves of the electrolysis in solutions containing different reactants are analyzed by use of an equivalent circuit model of a bipolar electrolyzer. The current corresponding to separate electrode reaction on the anodic or cathodic side of a bipolar plate is determined and the contribution of the currents connected with the oxidative degradation to the total current is discussed.

1. Experimental

The bipolar electrolyzer shown in **Fig. 1**, similar to the previous one,[6] was an acrylic cylindrical column 46 mm in inner diameter and 420 mm in height. As

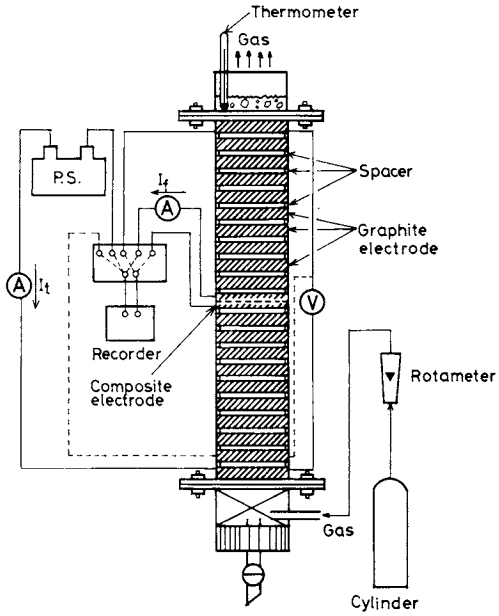

Fig. 1. Schematic diagram of apparatus

bipolar electrodes, two kinds of perforated graphite plates (EG-38), 46 mm in diameter and 10 mm thick, were used. One kind of plate had 12 holes of 6 mm diameter with square pitch and the other had 13 holes of the same diameter with right triangular pitch. Twenty-one electrodes were arranged by stacking the two kinds of plates alternately, each plate separated from the next by a 5 mm-thick spacer. A direct current flowed between the top and bottom plates as feeder electrodes at a constant voltage. The eleventh plate from the bottom was a composite electrode[6] for measuring the Faradaic current. The resistance of the electrolyte sandwiched between two bipolar plates was measured with an A.C. bridge at 1 kHz. In a separate experiment, the current flowed between the bottom plate and the second one from the bottom, and the current-voltage curve was measured. **Table 1** shows the electrolysis conditions of the solution components and sparged gases. Anodic oxidation of phenol without Fenton reaction was conducted in E1. A combined process of anodic oxidation and Fenton oxidation with hydrogen peroxide produced by cathodic reduction of oxygen was conducted in E2. To study the Faradaic current in detail, the electrolyses of E3–E5 were conducted. The pH value was adjusted to 2 with sulfuric acid and the electroconductivity of the electrolyte was adjusted to 0.45 $S \cdot m^{-1}$ with sodium sulfate. The electrolyte volume was 0.27 dm^3. Oxygen or nitrogen gas was introduced at $u_G = 1.4\,cm \cdot s^{-1}$ from the bottom into the column where liquid was treated in batch model. The experiments were conducted at 293 K. Chemical oxygen demand (COD) was measured with potassium dichromate. The present paper reports the results in the early stage of electrolysis, at less than 100 C.

Table 1. Electrolysis conditions and related electrode reactions

Abbrev.	Reactants	Gas	Electrode reactions (Eqs.)
E1	Phenol	Nitrogen	(4), (5) and (9)
E2	Phenol, Fe^{2+}	Oxygen	(4)–(9)
E3	None	Nitrogen	(5) and (9)
E4	Fe^{2+}	Nitrogen	(5), (6) and (9)
E5	Fe^{2+}	Oxygen	(5)–(9)

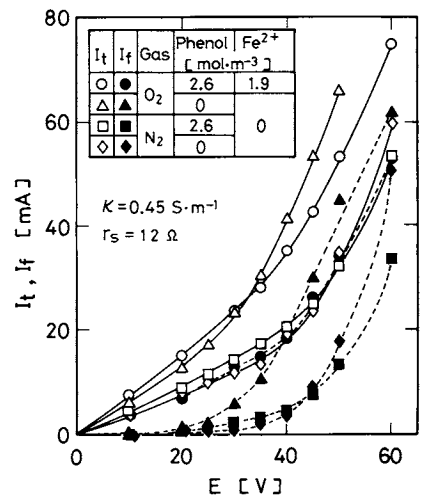

Fig. 2. Total current and Faradaic current at various cell boltages

Bipolar electrodes were pretreated with concentrated hydrochloric acid and nitric acid, and the electrolysis was carried out in sulfuric acid for half an hour before each experiment. After the experiment, the electrodes were washed with hot water.

2. Results and Discussion

2.1 Current-voltage curve

Figure 2 shows the total and Faradaic currents at different cell voltages. Since oxygen is reduced on the cathodic side of a bipolar plate, the total and Faradaic currents in the case of sparging oxygen are larger than those in the case of nitrogen gas. The relation between currents and cell voltage is affected by the electrode reactions on bipolar plates and feeder electrodes, and also by the electrolyte resistivity.

Figure 3 shows an equivalent circuit for the bipolar electrolyzer used in this work. The cell voltage E is expressed as follows.

$$E = E_a + (-E_c) + N_B E_B + (N_B + 1) r_s I_t \qquad (1)$$

where N_B, the number of bipolar plates, is 19, $E_a + (-E_c)$ the sum of the electrode potentials of feeder electrodes, E_B the electrode potential difference between opposite sides of a bipolar plate, r_s the resistivity and I_t the total current. In our previous paper,[6] it was assumed that the term $E_a + (-E_c)$ was

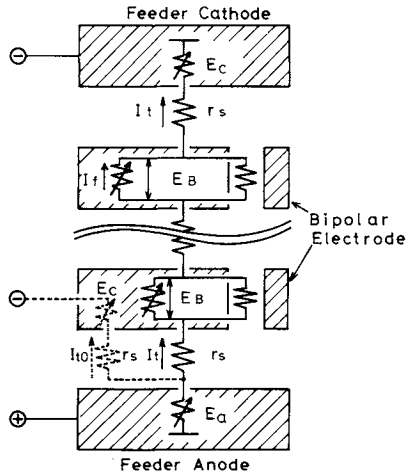

Fig. 3. Equivalent circuit model

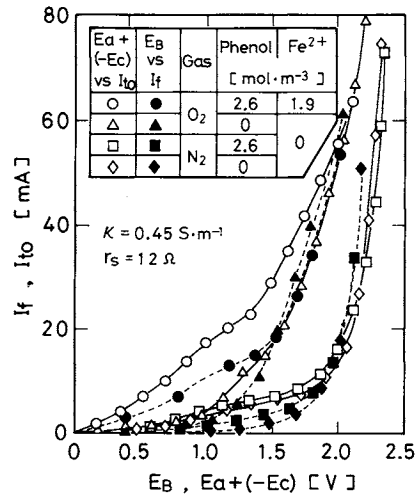

Fig. 4. Relations of I_{t0} to $E_a+(-E_c)$ and I_f to E_B

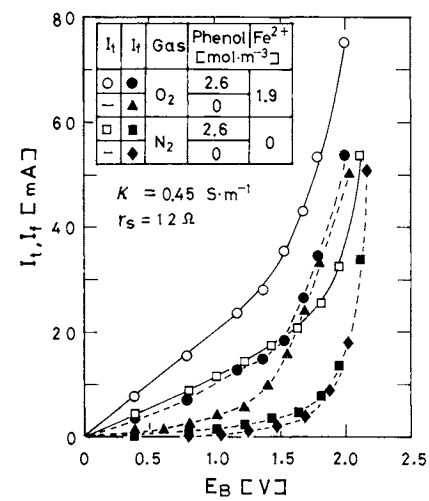

Fig. 5. Arrangement of relation of I_t and I_f to E_B

negligibly small compared to the other terms on the right-hand side of Eq. (1). The analysis assuming that $E_a+(-E_c)=E_B$ was also reported.[3] In the present paper, the value $E_a+(-E_c)$ was estimated from the current-voltage curve of electrolysis in the same electrolyte with two plates at the bottom and $E_a+(-E_c)$ was given by the following equation.

$$E_a+(-E_c)=E_0-r_sI_{t0} \tag{2}$$

where E_0 is the cell voltage and I_{t0} the total current for electrolysis with a pair of electrodes. By arranging Eq. (1), the E_B value is determined from the following equation.

$$E_B=[E-\{E_a+(-E_c)\}-(N_B+1)r_sI_t]/N_B \tag{3}$$

To obtain the E_B value, the function of $E_a+(-E_c)$ to I_t is required. The function of $E_a+(-E_c)$ to I_{t0}, determined from Eq. (2), was used instead of that of $E_a+(-E_c)$ to I_t.

Figure 4 shows the relations between I_{t0} and $E_a+(-E_c)$ and also between I_f and E_B. Both relations had similar tendencies but I_{t0} was larger than I_f. Since the feeder and bipolar electrodes have a certain thickness in the direction of current flow, strictly speaking the potentials of the solution phase in the pores of the two kinds of electrodes showed different profiles. The values of $E_a+(-E_c)$ and E_B were representative ones determined from an equivalent circuit model. The difference of two current-voltage curves might be affected by the actual potential profiles.

Figure 5 shows the relations of I_t and I_f to E_B in different solutions with sparging of oxygen or nitrogen gas. The total and Faradaic currents for sparging oxygen were larger than that for nitrogen gas at whole values of E_B. For sparging oxygen, the Faradaic current at $2.6\,mol\cdot m^{-3}$ of phenol concentration was larger than that without adding phenol, and the difference between the two currents was largest at about 1.1 V of E_B. For sparging nitrogen, the Faradaic current at $2.6\,mol\cdot m^{-3}$ of phenol concentration was a little larger than that without adding phenol.

2.2 Electrode reactions

Electrode reactions on both sides of a bipolar plate are shown by Eqs. (4)–(11).

On the anodic side:

$$C_6H_5OH=\text{Oxidized products}+ne^- \tag{4}$$

$$2H_2O=O_2+4H^++4e^- \tag{5}$$

$$Fe^{2+}=Fe^{3+}+e^- \tag{6}$$

On the cathodic side:

$$O_2+2H^++2e^-=H_2O_2 \tag{7}$$

$$O_2+4H^++4e^-=2H_2O \tag{8}$$

$$2H^++2e^-=H_2 \tag{9}$$

$$Fe^{3+}+e^-=Fe^{2+} \tag{10}$$

$$\text{Oxidized products}+ne^-=\text{Reduced products} \tag{11}$$

In the solution phase, the hydroxyl radical produced by Eq. (12) reacts with phenol and the Fenton reaction[1,10] proceeds.

$$Fe^{2+} + H_2O_2 = Fe^{3+} + OH^- + OH\cdot \qquad (12)$$

The Faradaic currents corresponding to anodic oxidation of phenol of Eq. (4) and cathodic reduction of oxygen to hydrogen peroxide of Eq. (7) are supposed to be effective in the oxidative degradation of phenol. The electrode reactions other than Eqs. (4) and (7) are side reactions, whose currents are desired to be small.

To discuss the contribution of Eqs. (4) and (7) to the Faradaic current, the $I_f - E_B$ curves for different experiments such as E1–E5 were analyzed and divided into anodic and cathodic parts with the following assumptions.

(1) The I_f values of Eqs. (5) and (9) were symmetrical with respect to the line of $E_r = 0.23$ V vs. Ag/AgCl.

(2) The apparent electrode potential of oxygen evolution was 1.2 V vs. Ag/AgCl.

(3) The currents corresponding to Eqs. (10) and (11) were small compared to the others.

(4) The currents of E1–E5 flowed according to the different combinations of Eqs. (4)–(9), as shown in Table 1.

The current-voltage curves respective to Eqs. (5) and (9) were evaluated from the $I_f - E_B$ curve of E3. The anodic and cathodic potentials, E_{ra} and E_{rc}, for a certain value of I_f were given by the following equations using assumption (1).

$$E_{ra} = E_B/2 + 0.23 \qquad (13)$$

$$E_{rc} = E_{ra} - E_B \qquad (14)$$

When several reactions occur on the electrode whose surface does not change during the electrolysis, the current is the sum of the separate currents of the reactions with respect to the electrode potential. Since the cathodic reaction of E1 was identical to that of E3, the cathodic part of the current-voltage curve of E1 was identical to that of E3. The anodic current I_f^* of E1 was determined as follows. The E_{ra} value for a certain value of I_f was given by the following equation, using the E_{rc} value on the cathodic part already determined and the E_B value determined from the $I_f - E_B$ curve of E1.

$$E_{ra} = E_{rc} + E_B \qquad (15)$$

A similar procedure was used to determine the anodic and cathodic currents of E2–E5. Using the fact that the cathodic current of E4 was identical to that of E3, the anodic part of the current-voltage curve of E4, which was identical to that of E5, was determined. On the basis of the anodic part of E5, the cathodic part of the current-voltage curve of E5, which was identical

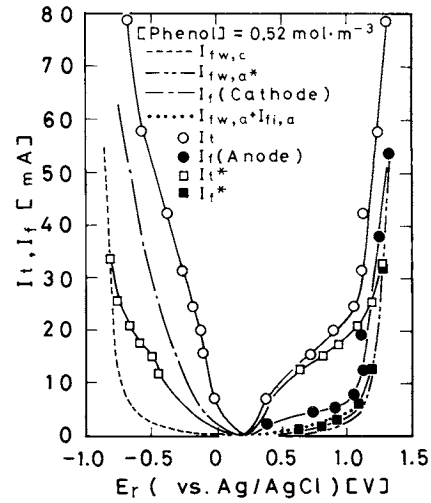

Fig. 6. Anodic and cathodic currents with respect to electrode potential at phenol concentration of 0.52 mol·m^{-3}

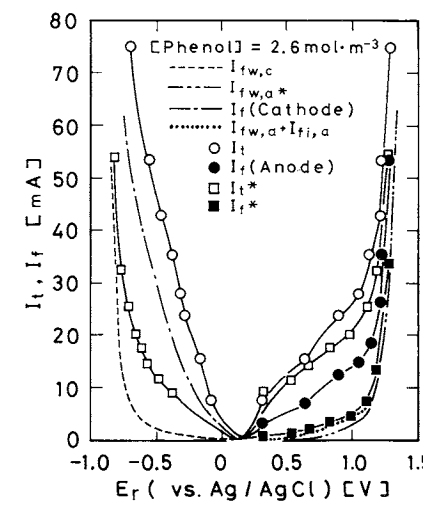

Fig. 7. Anodic and cathodic currents with respect to electrode potential at phenol concentration of 2.6 mol·m^{-3}

to that of E2, was determined. Then, on basis of the cathodic part of E2, the anodic part of E2 was determined.

Figures 6–8 show the relations of I_t and I_f to the electrode potentials of the anodic and cathodic sides. The anodic currents of Eqs. (5) and (6) and also the cathodic one of Eq. (9) are respectively indicated by $I_{fw,a}$, $I_{fi,a}$ and $I_{fw,c}$. In the case of E1 with nitrogen sparging, the superscript* is added to the character and the anodic current of Eq. (5) is indicated by $I^*_{fw,a}$. The apparent potential of oxygen evolution was obtained as 1.2 V, which was in agreement with assumption (2).

2.3 Contribution of Faradaic current to oxidative degradation

In the case of E1, only Eq. (4) is effective in the oxidative degradation of phenol. The contribution f_a^* of the current of Eq. (4) to I_t^* is expressed as follows.

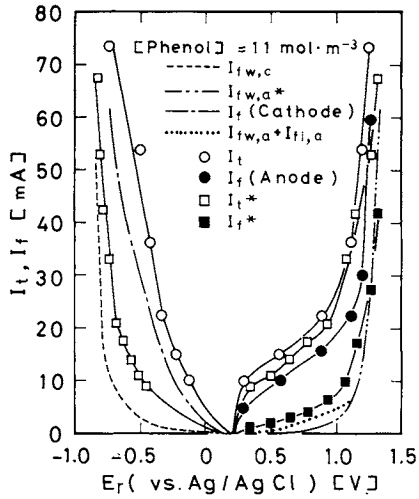

Fig. 8. Anodic and cathodic currents with respect to electrode potential at phenol concentration of 11 mol·m^{-3}

$$f_a^* = (I_f^* - I_{fw,a}^*)/I_t^* \times 100\% \quad (16)$$

In the case of E2, Eqs. (4) and (7) are effective in the oxidative degradation of phenol. Since it was difficult to obtain the currents of Eqs. (7) and (8) separately and the current efficiency for producing hydrogen peroxide was 50–70%[9] in the cathodic potential ranging from −2.0 V to −0.8 V at pH 2, the sum of the currents of Eqs. (7) and (8) was representative of the current of Eq. (7). The respective contributions f_a and f_c of Eqs. (4) and (7) to I_t are given by the following equations.

$$f_a = (I_f - I_{fw,a} - I_{fi,a})/I_t \times 100\% \quad (17)$$

$$f_c = (I_f - I_{fw,c})/I_t \times 100\% \quad (18)$$

2.4 COD current efficiency

The COD current efficiency Ce(COD) is defined by the following equation.

$$Ce(\mathrm{COD}) = (-\Delta\mathrm{COD})2FV/(16Q) \times 100\% \quad (19)$$

where $(-\Delta$COD) is the reduced value of COD, V liquid volume and Q the total coulombs. When Ce(COD) is 100%, the COD value decreases by 16 g per $2F$

Figure 9 shows the effect of E_B on Ce(COD) in experiment E1. The Ce(COD) value had its maximum value at an E_B value of about 1.7 V. Since the curves of Ce(COD) and f_a^* of Eq. (16) indicated similar tendencies to E_B, the oxidation efficiency η_a^* given by the following equation was determined by fitting the experimental value of Ce(COD) by the least square method.

$$Ce(\mathrm{COD})/(N_B+1) = \eta_a^* f_a^* \quad (20)$$

The value of η_a^* obtained was larger than unity so that COD might be reduced by reactions other than that of Eq. (4) such as dimerization[4] or the reaction of

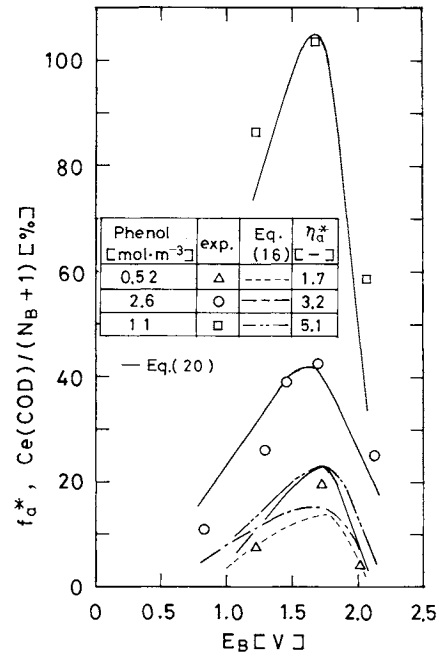

Fig. 9. Effect of E_B on COD current efficiency when sparging nitrogen gas

phenol with organic radicals.

Figure 10 shows the effect of E_B on Ce(COD) in experiment E2. The values of f_a and f_c, also shown in Fig. 10, had maximum values at E_B values of about 1.1 and 1.7 V respectively. The value of Ce(COD) was expressed by using oxidation efficiencies η_a and η_c.

$$Ce(\mathrm{COD}) = \eta_a f_a + \eta_c f_c \quad (21)$$

The solid lines in Fig. 10 were calculated from Eq. (21) using η_a and η_c determined by the least square method to fit the data. The Ce(COD) value showed a bimodal curve with respect to E_B except for a phenol concentration of 0.52 mol·m^{-3}. The values of f_a and f_c increased with increasing phenol concentration, but f_a was smaller than f_a^*. The Ce(COD) value of E2 increased with increment of phenol concentration and was larger than that of E1 over a wide range of E_B. The effect of sparging oxygen to generate Fenton's reagent was found to be useful for reducing COD.

Conclusion

The effect of electrode reactions of the anodic and cathodic sides on the oxidative degradation of phenol was examined in an undivided electrolyzer with the reactant solution sparged by nitrogen gas or oxygen gas. To clarify the contribution of the Faradaic current to the oxidative degradation, the Faradaic current was divided into anodic and cathodic parts by arranging the combination of electrode reactions in different experiments. The Ce(COD) value of E1 indicated a unimodal curve with respect to E_B. Meanwhile, since the contribution of the anodic

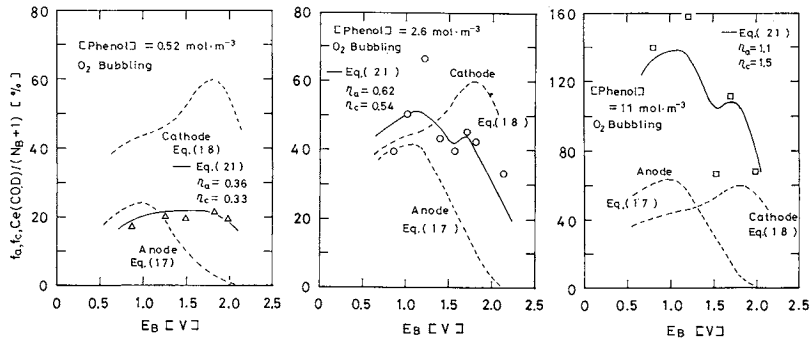

Fig. 10. Effect of E_B on COD current efficiency when sparging oxygen gas

current of phenol oxidation and the cathodic current of reduction of oxygen were respectively largest at about 1.1 and 1.7 V, the *Ce*(COD) value of E2 indicated a bimodal curve with respect to E_B.

Nomenclature

Ce(COD)	=	COD current efficiency	[%]
E	=	cell voltage	[V]
E_a	=	anodic potential of feeder electrode	[V]
E_B	=	electrode potential difference between opposite sides of a bipolar plate	[V]
E_c	=	cathodic potential of feeder electrode	[V]
E_r	=	electrode potential with respect to Ag/AgCl	[V]
F	=	Faraday's constant	[C·mol^{-1}]
f	=	contribution of current related to oxidative degradation to I_t	[%]
I_f	=	Faradaic current	[A]
I_t	=	total current	[A]
N_B	=	number of bipolar plates	[—]
n	=	charge number	[—]
Q	=	total coulombs	[C]
r_s	=	resistivity of sandwich solution	[Ω]
V	=	liquid volume	[m^3]
η	=	oxidation efficiency	[—]

〈Subscripts〉

a	=	anodic
c	=	cathodic
i	=	refers to Eq. (6)
w	=	refers to Eqs. (5) and (9)
0	=	electrolysis with a pair of electrodes

〈Superscript〉

*	=	experiment with sparging nitrogen

Literature Cited

1) Fenton, H.: *J. Chem. Soc.*, **65**, 899 (1894).
2) Gotoh, Y., N. Matsunaga, K. Doi and K. Azuma: *PPM*, **11** (12) 29 (1980).
3) Kusakabe, K., S. Morooka and Y. Kato: *J. Chem. Eng. Japan*, **19**, 43 (1986).
4) Shimizu, T., A. Kumagai and S. Nagaura: *Denki Kagaku*, **43**, 269 (1975).
5) Sudoh, M.: *Kagaku Kōgaku*, **51**, 417 (1987).
6) Sudoh, M., H. Kamei and K. Koide: *J. Chem. Eng. Japan*, **18**, 148 (1985).
7) Sodoh, M., H. Kitaguchi and K. Koide: *J. Chem. Eng. Japan*, **18**, 364 (1985).
8) Sudoh, M., H. Kitaguchi and K. Koide: *J. Chem. Eng. Japan*, **18**, 409 (1985).
9) Sodoh, M., T. Kodera, K. Sakai, J. Q. Zhang and K. Koide: *J. Chem. Eng. Japan*, **19**, 513 (1986).
10) Sudoh, M., T. Sasase, T. Yonebayashi and K. Koide: *Kagaku Kogaku Ronbunshu*, **11**, 70 (1985).

(Presented partly at the 52nd Annual Meeting of The Society of Chemical Engineers, Japan at Nagoya, April 1987.)